Electrospinning of *in-Situ* and *ex-Situ* Synthesised Polyimide Composites Reinforced by Titanate Nanotubes

Christian Harito, Ruben Porras, Dmitry V. Bavykin*, Frank C. Walsh

Energy Technology Research Group, Faculty of Engineering and the Environment, University of Southampton, University Road, Southampton, United Kingdom, SO17 1BJ

* Author for correspondence; D.Bavykin@soton.ac.uk

ABSTRACT

A colloidal dispersion of titanate nanotubes (TiNT) and polyamic acid (PAA) in dimethylformamide (DMF) was electrospun and chemically converted to polyimide (PI) - titanate nanotube (PI-TiNT) composite nanofibres of 500-1000nm diameter. The dispersion of nanotubes in the polymer was addressed by two different approaches, namely an i*n-situ* method (when TiNT was coated with one of the monomers) and an *ex-situ* one (when TiNT reacted directly with PAA). SEM images showed bead formation on samples from the *in-situ* approach*,* while *ex-situ* samples showed the absence of such features. Good distribution and some alignment of TiNT within the polymer fibres from *in-situ* or *ex-situ* approaches were observed by TEM imaging. Addition of titanate nanotubes into the polyimide significantly decreased the viscosity of polyamic acid solution and increased the glass transition temperature of the composite.

INTRODUCTION

Polyimide is a high performance polymer having excellent heat and chemical resistance combined with relatively facile processability, enabling it to be used in electronic devices, hot

gas filtration applications for spacecraft and in satellites[1,2]. The range of its applications can be expanded by the formation of micro and nanofibres of the polymer. Electrospinning is a facile and low-cost method to efficiently produce ultrathin fibres ranging from submicron to nanometre diameter. Such fine fibres can be tailored into the mat to achieve a tuneable volumetric porosity with a large surface to volume ratio. Moreover, a new functional composite material can be created by incorporating nanofiller into the nanofibres. For example, addition of Fe-FeO nanoparticles into polyimide nanofibres induces magnetic properties[3].

Since their discovery in 1997[4], titanate nanotubes have attracted much attention in applications which including hard ceramic fillers for soft polymers to improve mechanical and tribological properties[5]. Incorporation of elongated titanates into the polymers can also improve transport properties in nanofiltration membranes,[6] gas sorption capacity,[7,8] and corrosion resistance[7]. The benefits of TiNT combined with advanced properties of polyimide nanofibres could potentially extend their range of their application towards new functional medical textiles and UV protective clothing.

Achieving a uniform distribution of nanotubes within the polymer matrix has several associated difficulties. As prepared, TiNT are usually agglomerated into large bundles[8] caused by strong Van der Waals forces between them[9]; direct mixing of TiNT powders with the polymers tends to promote such agglomerates rather than isolated nanotubes in the polymer matrix. In contrast,

2

ulltrasonic treatment of the TiNT suspensions can successfully disintegrate such agglomerates, releasing single nanotubes. This process is also accompanied by the scission of nanotubes due to cavitation, resulting in a reduction in their length[10,11]. Modification of the nanotube surface is a promising approach for facilitation of TiNT release into the solution without breaking of the nanotubes, which can improve the stability of the TiNT aqueous colloidal suspension[12]. There are few methods for effective dispersion of TiNT in a polar organic solvent, in which most polymer materials are industrially prepared.

Due to the relatively high viscosity of polymer solutions and the long length of the polymer chains, a uniform dispersion of isolated nanostructures within the matrix can only be achieved by extended mixing or ultrasonication. Alternatively, a method can be adopted in which polymer is synthetized in the presence of nanostructured materials[13]. In the case of polyimide, synthesis is usually performed in two stages which can be realised in two ways. An *in-situ* approach involves interaction of one of the monomers with TiNT prior to polymerization. In an *ex-situ* approach, TiNT is introduced to the intermediate polyamic acid. In both methods, good interaction between TiNT and molecules containing the -NH_2 group is anticipated, which can promote better dispersion by preventing coagulation of nanostructures.

Studies incorporating titanate nanotube into electrospun fibre are still very limited. Bajsić, *et. al.* [14] have embedded titanate nanotubes and TiO_2 nanospheres into electrospun

3

polycaprolactone. However, the work mainly considered the effect of added filler on the UV stimulated degradation of the polymer composite fibres, without detailed investigation of the distribution of filler within the polymer. From our previous experience, good uniformity of filler dispersion in the polymer can strongly affect its mechanical performance and other properties. In the present work, we have studied the electrospinning of polyamic acid mixed with suspended cetyltrimethylammonium bromide (CTAB) coated titanate nanotubes in dimethylformamide (DMF) solution with the aim of producing TiNT reinforced polyamide composite nanofibres. Both *ex-situ* and *in-situ* approaches have been investigated. It was found that viscosity of the polyamic acid solution containing added TiNT depends on the method of mixing, which also greatly affects the quality of the electrospun fibres. Optimization of all experimental conditions allowed preparation of polyimide nanofibres with an average diameter ranging between 500 and 1000 nm. Inside the body of these microfibers, embedded titanate nanotubes were evenly distributed within the polymer matrix and, to an extent oriented parallel to the fibre direction, as observed by SEM and TEM. The effect of the added titanate nanotube on thermal property of polyimide composite is also discussed.

EXPERIMENTAL DETAILS

Reagents and materials

The TiNT was prepared using our previously developed reflux methodology in an aqueous solution of mixed KOH and NaOH.[15] The length and outer diameter of titanate nanotube were above 100 nm and ca 25 nm, respectively. 4,4'-oxydianiline (ODA, 97%), pyromellitic

dianhydride (PMDA, 97%), cetyltrimethylammonium bromide (CTAB, 95%), acetic anhydride, pyridine, N,N-dimethylformamide (DMF) were supplied from Sigma-Aldrich and used without purification.

Preparation and electrospinning of pure polyimide fibre

A mixture of 2.392 g of ODA (1 mol) and 20 g of DMF was stirred in a 250 cm^3 round bottom flask at 22±2.5 ^{o}C. After the ODA had dissolved, 2.608 g of PMDA (1 mol) was added to the solution followed by stirring for 2 days, yielding 20 wt% DMF solution of polyamic acid. All the reactions were shielded by a nitrogen gas blanket. The solution was transferred into a syringe for electrospinning. A solution of polyamic acid in DMF was spun to an aluminium foil collector at a distance of 20, 25, 30, and 35 cm via a 20 kV DC voltage with a relative humidity level of 40±5%. Finally, the fibre was immersed in a mixture of acetic anhydride and pyridine (4 : 3.5 volume ratio) for 1 min, followed by heating at 120 ^{o}C for 1 h.

Preparation of CTAB-coated titanate nanotube colloidal suspension

2.5 g of titanate nanotubes were stirred with 5 cm^3 of 0.1 M CTAB and 25 cm^3 distilled water for 3 days. Titanate nanotubes were separated from the solution and dried at 22±2.5 ^{o}C under vacuum. For preparation of the colloidal solution, 2 g of CTAB-coated TiNT was stirred in 1 dm^3 DMF for 2 weeks at 600 rpm. The solution was allowed to settle for 48 h and the top of the liquid was collected yielding stable colloidal suspension (240 mg dm^{-3}, measured by a gravimetric method).

Preparation of *in-situ* polyimide-titanate nanotube fibre

2.391 g of 4,4'-oxydianiline (ODA) was mixed with 20 g of a stable colloidal suspension of CTAB-coated TiNT in DMF (240 mg dm^{-3}) stirred at 22±2.5 ^{o}C. After ODA had dissolved, 2.604 g of pyromellitic dianhydride (PMDA) (equimolar with ODA) were added to the solution and stirred for 2 days, yielding 20 wt% DMF solution of *in-situ* polyamic acid-titanate nanotube composite. All the polymerisation reactions took place in a nitrogen atmosphere. The solution of PAA-TiNT was electrospun to the aluminium foil collector at a distance of 20 cm with a 20 kV DC voltage. The solution was supplied to the 0.8 mm needle using a syringe pump (IME Technologies, Netherlands) at a pumping rate 0.12 cm^3 h^{-1}. In order to dehydrate the polyamic acid and convert it to polyimide, the electrospun PAA fibres were immersed in a mixture of acetic anhydride and pyridine (4 : 3.5 volume ratio) for 1 min followed by heating in oven at 120 ^{o}C for 1 h.

Preparation of *ex-situ* polyimide-titanate nanotube fibre

2.391 g of ODA was stirred in 10 g of DMF until complete dissolution. 2.604 g of pyromellitic dianhydride (PMDA) (equimolar with ODA) were added to the solution and stirred for 1 day, to produce a viscous solution of polyamic acid. 20 g of stable, colloidal suspension of CTAB-coated titanate nanotube in DMF (240 mg dm^{-3}) was concentrated by rotary evaporation at 120 ^{o}C, yielding 10 g of concentrated stable colloidal suspension (480 mg dm^{-3}). The concentrated solution was slowly poured into a viscous polyamic acid solution and stirred for 1 day. To produce the fibre, a solution of *ex-situ* synthesized polyamic acid-titanate nanotubes was spun onto an aluminium foil collector using a 20 kV DC voltage at a distance of 20 cm from the

syringe tip. The solution was fed to the 0.8 mm needle by a syringe pump (IME Technologies, Netherlands) at a pumping rate of 0.2 cm^3 h^{-1}. Finally, the PAA/TiNT fibre was immersed in a mixture of acetic anhydride and pyridine (4:3.5 volume ratio) for 1 min followed by continued heating in air at 120 ^{o}C for 1 h. Figure 1 schematically shows the details of both *ex-situ* and *in-situ* approaches.

Materials Characterisation

FESEM images were taken by a JEOL JSM 6500F microscope at an accelerating voltage of 5 or 15 kV. The supernatant from the colloidal suspension was diluted and cast as 100 µl drops onto a silicon wafer which had been cleaned with acetone. The fibre was electrospun on the top of a silicon wafer for 15 minutes then its morphology was characterised by SEM imaging. The diameter of titanate nanotubes and electrospun fibres was determined by 100 measurements.

TEM images of TiNT/PI or TiNT/PAA composite fibres were acquired using a JEOL 3010 transmission electron microscope at an accelerating voltage of 300 kV with an exposure time of 1 second. To prepare a specimen, DMF solutions of PAA or TiNT/PAA were electrospun for 1 min on the copper grids coated with perforated carbon film, followed by dehydration of the composite in a mixture of acetic anhydride and pyridine (4 : 3.5 volume ratio) for 1 min.

A Fourier transform infrared spectrometer (Nicolet 380 FT-IR Spectrometer, Thermo Scientific) was used to characterise samples at a resolution of 4 cm^{-1}. For each sample, 32 successive scans were recorded over the wavenumber region of 500-4000 cm^{-1}. To smooth the FTIR spectra, a

Savitzky-Golay filtering algorithm was used. The viscosity of titanate nanotubes-polyamic acid solution was evaluated by a CAP 2000+ viscometer.

Thermal characterization of pure polyimide (PI) and PI/TiNT composite (14.2-20.5 mg) was performed by a Pyris 1 (Perkin Elmer) differential scanning calorimeter (DSC) under nitrogen atmosphere. Pristine polyimide and PI/TiNT composite films were cut to provide a snug fit into the holder. Each sample was held for 1 min at 50 ^{o}C then heated from 50 to 500 ^{o}C at the rate of 10 ^{o}C min^{-1}. The temperature was held at 500 ^{o}C for 1 min then allowed to cool to 30 ^{o}C before a sample was removed from the holder.

RESULTS AND DISCUSSION

Electrospinning of polyimide microfibre

Although polyimide materials have been widely used in industrial applications[1, 2], electrospinning of the polymer solution into microfibers was challenging, due to the low solubility of the polyimide in most common solvents. Following recent improvement of the electrospinning technique and identification of proper solvents, the effect of various parameters such as polymer humidity[16], concentration and applied voltage[17] on the properties of electrospun polyimide has been studied. It was established that polymer concentration must be higher than 10 wt% to maintain a stable jet, creating bead-free uniform smooth and continuous fibre. Water molecules in the air influence the discharge rate and the electrical conductivity of the fibre surface. Reducing humidity produces a smaller diameter of fibre. As a

result, ultrafine polymer fibre ≈100 nm can be produced under a relative humidity of 5%. A stronger electrical field, achieved by increasing applied voltage, can induce more uniform and smooth fibres due to stretching of the polymer jet during electrospinning. The effect of working distance, however, has not been systematically studied for PI microfibres.

Generally, increasing the distance from the tip of the needle to the collector is equivalent to a lower applied voltage, which can cause less stretching forces on the jet of the liquid resulting in wider diameters of the obtained fibres. It can also increase the diameter since a longer distance means a longer flight time of the polymer jet before deposition. Working distances which are too short or too long can cause jet instability, resulting in appearance of beads or total disappearance of fibres, respectively[18].

It was shown elsewhere[20] that there was no significant change in fibre morphology upon changing the working distance from 10 cm to 20 cm. In order to better understand the effect of working distance, we have extended it from 20 cm to 35 cm during electrospinning of PAA solutions. Figure 2 shows SEM images of PI microfibres electrospun with the working distance set to 20, 25, 30, and 35 cm, while constant values have been applied to other parameters (20 kV applied voltage, 0.1 cm^3 h^{-1} feed rate, 20 wt% polymer solution, humidity 40±5%). It was found that the diameter of the fibres is almost linearly grown with larger working distance between 25 and 35 cm (see Figure 3) indicating that (i) jet is stable at these conditions and (ii)

follows general trend associated with less stretching under weaker electric field. Further expansion of the working distance (>35 cm) can enlarge the diameter of polyimide fibre but it can also induce more inhomogeneity of the fibre due to lowered jet stability. Indeed, Figure 2d shows that the fibres are characterised by more frequent bending, compared to those achieved at shorter distances. A similar tendency was seen in a experiment using a relatively high polycaprolactone concentration (7.5 and 10 wt%) in acetone solution at a low flow rate of 0.05 cm^3 min^{-1} [19].

Due the low solubility of polyimide materials in many solvents, it is more practical to work witha polyamic acid which is precursor of PI has better solubility in most solvents. Imidization is a process that irreversibly converts polyamic acid (PAA) to polyimide (PI) through cyclization and dehydration catalysed by water binding chemicals or by the thermal treatments. A mixture of the acetic anhydride and pyridine was employed to convert polyamic acid to polyimide fibre. Acetic anhydride acts as a dehydrating agent, since the pyridine works as a base catalyst.

FTIR spectra show that one minute immersion in acetic anhydride and pyridine (4: 3.5 volume ratio) followed by heating at 120 ^{o}C for 1 hour results in conversion of polyamic acid to polyimide (see Figure 4). The peak at 1660 cm^{-1} can be assigned to strong absorption of carbonyl (C=O) stretching of the amide group and the band at 1550 cm^{-1} is probably due to C–NH stretching vibration. The broad peak around 3500 cm^{-1} is associated with N-H and O-H stretching in polyamic acid. The disappearing of this broad peak after chemical imidization indicates successful cyclisation of N-H and O-H to the

imide group. Moreover, new polyimide peaks are observed in fingerprint region: 1780 cm^{-1}, 1720 cm^{-1}, 1380 cm^{-1}, and 723 cm^{-1} corresponding to C=O symmetric stretching vibration, C=O asymmetric stretching vibration, C–N stretching vibration, and C=O bending, respectively. Similar changes in the FTIR spectra have been observed elsewhere[20], during the conversion of polyamic acid to polyimide.

Figure 5 shows SEM images of electrospun PAA fibres before and after chemical imidization. Unlike the thermal imidization in which the fibres usually shrink with a lower average diameter[21], we have found that, during chemical imidization, the average diameter increased from 210±70 nm to 502±100 nm (see Figure 5), probably due to swelling caused by the dehydrating agents. Neat polymer fibres tended to kink and intertwine with each other after chemical imidization. The reasons for such deformations of the fibres during imidization, according to Nishino *et. al*[22], are internal mechanical stress, arising from chemical processes and thereluctance of long polymer chains to allow relaxation and stress relief.

Synthesis of *in-situ* and *ex-situ* polyimide/titanate nanotube composite microfibres

Since blending of titanate nanotubes with polymer occurs in colloidal solution, it is necessary to established stable colloidal suspension of TiNT for at least the duration of polymerisation and evaporation of the solvent. Due to the anionic nature of TiNT, they tend to develop a negative zeta potential in aqueous suspensions, stabilizing the colloidal solution of TiNT. In many organic

aprotic solvents, however, such a mechanism of stabilization does not occur. Recently, we have found that CTAB coated TiNT can be suspended in polar aprotic solvents (chloroform) by long term stirring[11]. FTIR spectra (see Figure 6) indicate the strong adsorption of CTAB on the surface of nanotubes, probably due to interaction between -OH groups in TiNT and $-NR_4^+$ groups in CTAB. New peaks appeared at 2835 cm^{-1} and 2915 cm^{-1}, which can be related to the C-H stretching oscillations in $-CH_2$ groups, whereas two peaks at 1150 cm^{-1} and 1250 cm^{-1} are probably linked to N-C stretching oscillation in the tertiary ammonium ion $-NR_4^+$ of CTAB molecule, suggesting that titanate nanotubes have been covered by adsorbed CTAB.[23] In this work, we report for the first time that such an approach also allows dispersion of TiNT in DMF solvent and formation of stable suspension of isolated nanotubes. Figure 7 shows an SEM image of isolated as well as agglomerated nanotubes deposited on a silicon wafer from a colloidal solution of CTAB coated TiNT in DMF. The typical diameter of TiNT is ca 20 nm. Although the SEM image shows the presence of some nanotubes bundles, they are less compact than the large agglomerates in the powdered TiNT sample. This indicates that, in colloidal solutions, most of the nanotubes are isolated. The long hydrophobic $-CH_2-$ chain of CTAB molecules not only gives rise to steric hindrance between adjacent titanate nanotubes, dispersing them in DMF but also may improve interactions between nanotubes and the hydrophobic polymer molecules.

This stable colloidal solution of TiNT in DMF has been further used in both *in-situ* and *ex-situ* approaches for blending polymer with the inorganic nanostructures (see Figure 1). The resulting

mixture was used for electrospinning of PAA-TiNT microfibers. After analysis of literature and taking into account our studies of electrospinning of pure PAA, we have selected optimal operational conditions for electrospinning of the composite, which are 20 kV of applied voltage, 20 cm working distance, 40±5 % of humidity, and 20 wt% of PAA in the DMF solution.

Addition of titanate nanotubes into polyamic acid solution significantly reduced the dynamic viscosity. For example, the measured viscosity of the 20 wt% solution of PAA in DMF was ≥10000 mPa.s at room temperature 298 K), whereas a small addition of TiNT (only 0.1 wt% of total solid) has resulted in a decrease in the viscosity to 3840 mPa s and 2870 mPa s for *ex-situ* and *in-situ* TiNT-polyamic acid, respectively. Usually, addition of nanostructured materials to the diluted solution of polymer results in linear (in respect to concentration of added nanoparticles) growth of its dynamic viscosity[24]. However, deviations from that tendency have been widely observed recently[25 - 28]. Jain's selective adsorption hypothesis[28] is probably the most relevant effect here. Long and high molecular mass polyamic acid chains are selectively absorbed on the surface of titanate nanotube, leading to reduction in entanglement between polymer chains in the solutions thus lowering apparent dynamic viscosity. Additionally, the CTAB molecules desorbed from the TiNT can potentially disrupt hydrogen bonding between carboxylic groups in polyamic acid ionomer rendering less interaction between polymer chains[29]. Due to the fact that both *in-situ* and *ex-situ* composite mixtures showed a reduction in viscosity, we can rule out the possibility that such a reduction is due to inhibition of the

polymerisation in presence of TiNT. Indeed, for the *ex-situ* case, the polyamic acid is fully formed before the addition of nanotubes.

Generally, for efficient electrospinning of polymer solutions into the desired quality nanofibres the rheological properties of the solutions (such as viscosity, surface tension, electric conductivity, volumetric charge density, etc.) could vary only within the certain limits extending of which may result in instability of the electrically charged jet leading to formation of beads or wide distribution in nanofibres diameters.[30] However, the observed reduction in viscosity after addition of TiNT has facilitated pumping of the dissolved polymer mixture during electrospinning.

Viscosity differences between *In-situ* and *ex-situ* synthesis conditions affected the morphology of the composite fibre. Figure 8b shows frequent occurrence of the polymer beads with a typical size of 188±80 nm in the nanofiber direction, with a typical diameter of 57±20 nm PAA/TiNT composite prepared by the *in-situ* method in which viscosity of the electrospinning fluid was 2870 mPa s. In contrast, electrospinning of the PAA-TiNT solution of the same concentration prepared by *ex-situ* methods with 3840 mPa s viscosity results in larger diameter of composite nanofibres (328±93 nm) with no bead formation (see Figure 8a).

These observations are in agreement with previously observed effects of the viscosity of electrospinning fluids on the probability of bead formation[31]. At low viscosity, beaded fibre is usually formed by capillary break-up of the jet during electrospinning. Since a higher concentration of polymer in solution results in an increased viscosity,[32] the quality of the *in-situ* synthesised fibres could be improved by increasing the concentration of PAA.

In order to determine the distribution of nanostructured TiNT within the polymer fibres HR-TEM was employed. Our early samples in which colloidal solution of nanotubes was prepared by 1 day stirring of the TiNT powder in DMF show poor dispersion of nanotubes which remain aggregated in original unbroken particles (see Figure 9a) resulting in appearance of random swellings in the uniform nanofibre in SEM images. Despite poor dispersion, TEM image confirms good interaction between TiNT and polyimide seeing as efficient wetting of the nanotubes by polymer. It appears that all of the nanotubes are covered by polymer materials meaning that poor dispersion is mainly due to the presence of initial TiNT agglomerates in the colloidal solution.

Using our previously established method of untangle nanotubes agglomerates without shortening of their length by long term stirring[11], the colloidal solution of isolated TiNT obtained by 2 weeks stirring was used for preparation of PI/TiNT composite nanofibres. Figures 9c and 9d shows TEM image of polyimide nanofibres reinforced by titanate nanotubes prepared by *ex-situ*

and *in-situ* respectively. Both samples show the appearance of nanotubes oriented along the length of the fibre. From the analysis of many TEM images it was concluded that (*i*) despite absence of large agglomerates of TiNT, the observed nanotubes are mostly found assembled into small bundles, (*ii*) there are long fragments of the fibres completely free from the nanotubes and (*iii*) in case of low viscosity *in-situ* solution, there are appearance of spheroidal beads without embedded nanotubes (see Figure 9b). It is possible that aggregation of nanotubes into the small bundles occurs during electrospinning when the fluid passes through electrostatically charged needle. When such solution of PAA and TiNT was used for preparation of film composite by casting, the uniform distribution of nanotubes within the polymer was observed (not shown here). Since the quantity of the added nanotubes is still relatively low and the distribution of TiNT is not completely uniform, nanofibers, rather than nanotubes, are seen. The appearance of empty beads of polymer (Figure 9b) suggests that their formation was primarily associated with low fluid viscosity rather than the presence of large TiNT agglomerates (Figure 9a).

The thermal properties of PI-TiNT fibres have been further investigated using differential scanning calorimetry (DSC), which is a common method to determine the glass transition temperature (T_g) of polymer. Usually, T_g can be detected by the baseline shift or a peak in the DSC curve indicating an endothermic processes linked to rapid change in polymer mobility from glassy to rubbery state. The DSC curve of pure, neat polyimide fibres shows a characteristic endothermic peak at 407 ºC of relatively narrow width, which can be associated with glass

transition (see Figure 10a). The reported T_g for pure ODA-PMDA polyimide is within that range of temperatures[33].

Addition of nanostructures into the polymer matrix can either increase or decrease the T_g of polymer composite depending on the mechanism of interactions between nanoparticles and polymeric chain[34]. We have found that small addition of titanate nanotubes (0.1 wt%) to the PI matrix, obtained by both *in-situ* and *ex-situ* methods, has increased its T_g by *ca.* 70 ^{o}C from 407 ºC to 477 ºC (Figure 10). Such a dramatic shift in T_g is not unusual for PI polymers. Recently it has been reported 50 ºC shift of T_g temperatures in polyimide − graphene composite[35]. The mechanism involved in the change of glass transition is probably related to the strong interaction between nanostructured titanates and polyimide resulting in more restriction in polymer chains mobility via steric hindrance. Also, strong covalent bond may occur between hydroxyl group on the surface of titanate nanotube and amino group of polyamic acid during imidization resulting in branching the polymer chain and leading to cross-linking, which usually increases the glass transition temperature in polyimide [36].

Addition of nanostructured material to the monomers during polymerization can affect the degree of polymerization of the final polymer to such a degree that the T_g of polymer nanocomposite is altered[37]. However, we have found that the T_g is the same in both *in-situ* and *ex-situ* composites (see Figure 10b and Figure 10c) proving that addition of titanate nanotube

17

does not affect the degree of PAA polymerisation. Usually, an *in-situ* type approach to dispersion of inorganic nano- and micro- particles into polymer matrix gives better results compared to *ex-situ methods*[13]. In the present work, however, both approaches resulted in a satisfactory distribution of nanotubes in the polymer, allowing greater flexibility in the production of composites.

CONCLUSIONS

Nanofibres of polyimide - titanate nanotube composite have been successfully synthesized by electrospinning. CTAB coating of the nanotubes was essential for preparation of isolated titanate nanotubes in DMF. The addition of titanate nanotube greatly decreases the viscosity of polyamic acid (as a polyimide precursor). The reduction of viscosity reduces the production of kinked and intertwined fibre after chemical imidization. This lowering of viscosity may be caused by selective absorption of high molar mass polyamic acid on titanate nanotubes, leading to a reduction in entanglement density and an improvement in chain mobility. However, beads occur on the composite fibre at very low viscosity (2870 mPa s) suggesting that higher viscosity is beneficial to creation of bead-free nanofibres. Several approaches have been employed to prepare aligned titanate nanotube within polyimide fibres. This work recommends the use of a stable colloidal suspension, whether concentrated (as used in *ex-situ* samples) or not (as used for *in-situ* samples), to synthesise an aligned titanate nanotube within polyimide fibre. A significant increase in the glass transition temperature of polyimide was observed after the incorporation of a small amount of titanate nanotubes, which probably strongly interact with

the polyimide chains and restricted their mobility. Strong covalent bonding may occur between hydroxyl groups on the surface of titanate nanotubes and the polyamic acid during imidization causing some degree of cross-linking in polyimide.

ACKNOWLEDGEMENTS

REFERENCES AND NOTES

1. Liaw, D.J.; Wang, K.L.; Huang, Y.C.; Lee, K.R.; Lai, J.Y.; Ha, C.S. *Prog. Polym. Sci.*, **2012**, *37*, 907–974.

2. Watson, K.A.; Palmieri, F. L.; Connell, J. W. *Macromolecules*, **2002**, *35*, 4968–4974.

3. Zhu, J.; Wei, S.; Chen, X.; Karki, A. B.; Rutman, D.; Young, D. P.; Guo, Z. *J. Phys. Chem. C*, **2010**, *114*, 8844–8850.

4. Kasuga, T.; Hiramatsu, M.; Hoson, A.; Sekino, T.; Niihara, K. *Langmuir*, **1998**, *14*, 3160–3163.

5. Bavykin, D. V.; Walsh, F. C. In Titanate and Titania Nanotubes: Synthesis, Properties, and Applications; Royal Society Chemistry, Cambridge, **2010**.

6. Sumisha, A.; Arthanareeswaran, G.; Ismail, A.F.; Kumar, D.P.; Shankar, M.V.; *RSC Adv.*, **2015**, *5*, 39464-39473.

7. Herrasti, P.; Kulak, A.N.; Bavykin, D.V.; Ponce de Léon, C.; Zekonyte, J.; Walsh, F.C. *Electrochim. Acta.,* **2011**, *56*, 1323-1328.

8. Ma, P. C.; Siddiqui, N. A.; Marom, G.; Kim, J. K. *Compos. Part A- Appl. Sci.,* **2010**, *41*, 1345-1367.

9. Girifalco, L. A.; Miroslav, H.; Lee, R. S. *Phys. Rev. B,* **2000**, *62*, 13104.

10. Zennaro, L.; Magro, M.; Vianello, F.; Rigo, A.; Mariotto, G.; Giarola, M.; Froner, E.; Scarpa, M. *Chem. Phys. Chem.,* **2013**, *14*, 2786–2792.

11. Ortigosa, R.P.; Bavykin, D.; Zekonyte, J.; Walsh, F.; Wood, R. *Nanotechnol.*, **2016**, *27*, 195706-195716.

12. Papa, A.L.; Boudon, J.; Bellat, V.; Loiseau, A.; Bisht, H.; Sallem, F.; Chassagnon, R.; Bérarda, V.; Millot, N. *Dalton Trans.,* **2015**, *44*, 739-746.

13. Sain, S.; Bose, M.; Ray, D.; Mukhopadhyay, A.; Sengupta, S.; Kar, T.; Ennis, C. J.; Rahman, P. K.; Misra, M. *Journal of Reinforced Plastics and Composite*, **2013**, 32, 147–159.

14. Bajsić, E.G.; Mijović, B.; Penava, N.V.; Grgurić, T.H.; Slouf, M.; Zdraveva, E. *J. Appl. Polym. Sci.,* **2016**, *133*, 43539.

15. Bavykin, D. V.; Kulak, A. N.; Walsh, F.C. *Cryst. Growth Des.,* **2010**, *10*, 4421–4427.

16. Fukushima, S.; Karube, Y.; Kawakami, H. *Polymer Journal*, **2010**, *42*, 514–518.

17. Liu, J.; Huang, J.; Wujcik, E.K.; Qiu, B.; Rutman, D.; Zhang, X.; Salazard, E.; Wei, S.; Guo, Z. *Macromol. Mater. Eng.*, **2015**, *300*, 358–368.

18. Mazoochi, T.; Hamadanian, M.; Ahmadi, M.; Jabbari, V. *Int. J. Ind. Chem.*, **2012**, 3, 2.

19. Bosworth, L.A.; Downes, S. *J. Polym. Environ.*, **2012**, *20*, 879.

20. Nah, C.; Han, S.H.; Lee, M.H.; Kim, J.S.; Lee, D.S. *Polym. Int.*, **2003**, *52*, 429.

21. Yang, K.S.; Edie, D.D.; Lim, D.Y.; Kim, Y.M.; Choi, Y.O. **Carbon**, 2003, *41*, 2039–204.

22. Nishino, T.; Kotera, M.; Inayoshi, N.; Miki, N.; Nakamae, K. *Polymer*, **2000**, *41*, 6913-6918.

23. Zhang, M.; Wu, Y.; Feng, X.; He, X.; Chen, L.; Zhang, Y. *J. Mater. Chem.,* **2010**, *20*, 5835-5842.

24. Hughes, A.J. *Nature*, **1954**, *173*, 1089-1090.

25. Jain, S.; Goossens, J.G.P.; Peters, G.W.M.; van Duin, M.; Lemstra, P.J. *Soft Matter*, **2008**, *4*, 1848–1854.

26. Tuteja, A.; Mackay, M.E.; Hawker, C.J.; van Horn, B. *Macromolecules*, **2005**, *38*, 8000-8011.

27. Kalathi, J.T.; Grest, G.S.; Kumar, S.K. *Phys. Rev. Lett.*, **2012**, *109*, 198301.

28. Mackay, M.E.; Dao, T.T.; Tuteja, A.; Ho, D.L.; Horn, B.V.; Kim, H.C.; Hawker, C.J. *Nature Materials*, **2003**, *2*, 762-766.

29. Zhang, L.; Brostowitz, N.R.; Cavicchi, K.A.; Weiss, R.A. Macromol. *React. Eng.*, **2014**, *8*, 81–99.

30. Reneker, D.H.; Yarin, A.L.; Fong, H.; Koombhongse, S. *J. Appl. Phys.*, **2000**, *87*, 4531-4547.

31. Fong, H.; Chun, I.D.; Reneker, H. *Polymer*, **1999**, *40*, 4585-4592.

32. Chisca, S.; Barzic, A.I.; Sava, I.; Olaru, N.; Bruma, M. *J. Phys. Chem. B*, **2012**, *116*, 9082–9088.

33. Bershtein, V.A.; Sukhanova, T.E.; Krizan, T.D.; Keating, M.Y; Grigoriev, A.I.; Egorov, V.N.; Yakushev, P.N.; Peschanskaya, N.N.; Vylegzhanina, M.E.; Bursian, A.E *J. Macromol. Sci., Part B: Phys.,* **2005**, *44*, 613-639.

34. Corcione, C.E.; Frigione, M. *Materials*, **2012**, *5*, 2960-2980.

35. Marashdeh, W.F.; Longun, J.; Iroh, J.O. *J. Appl. Polym. Sci.*, **2016**, 43684.

36. Kim, K.; Yoo, T.; Kim, J.; Ha, H.; Han. H. J. *Appl. Polym. Sci.*, **2014**, 41412.

37. Lanciano, G.; A. Greco, A. Maffezzoli, M.L. *Thermochim. Acta*, **2009**, *493*, 61–67.
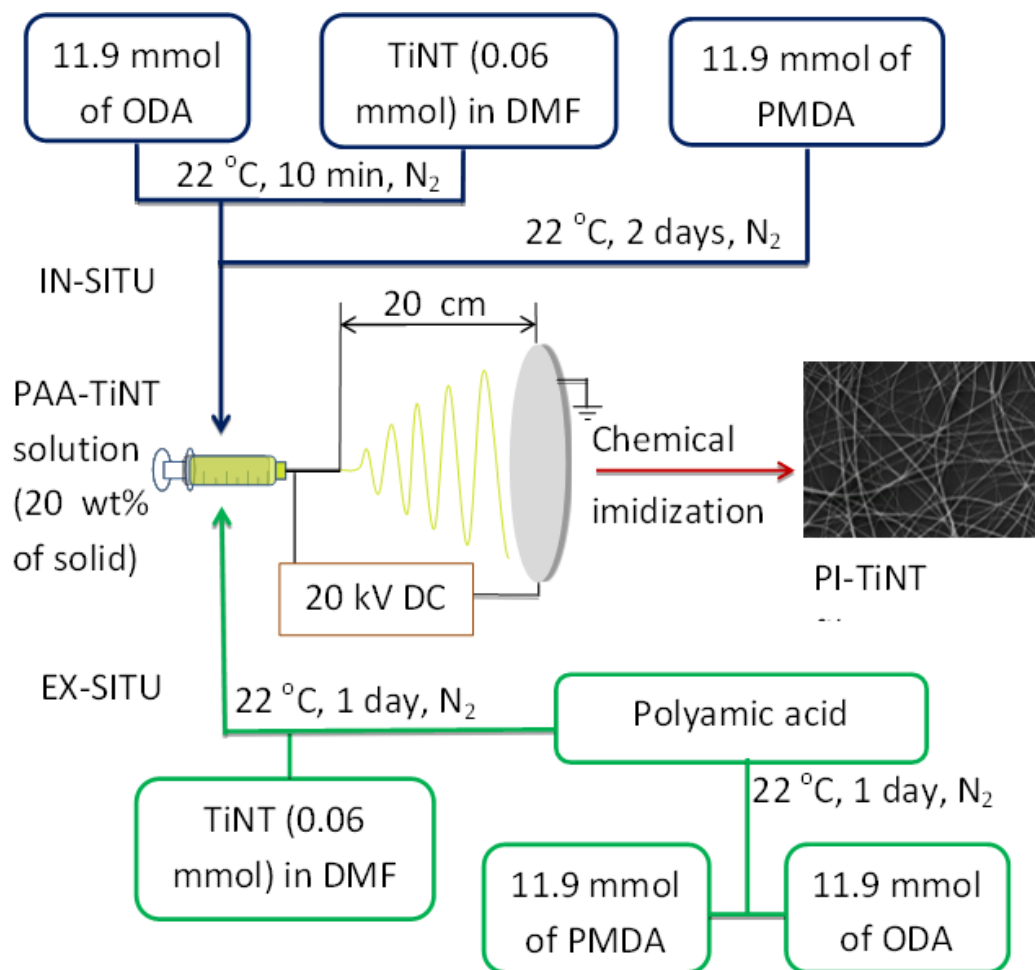
Figure 1. Schematic illustration of electrospinning of *in-situ* and *ex-situ* polyamic acid-titanate nanotube (PAA-TiNT) nanofibres. For chemical imidization, the PAA-TiNT fibres collected on the aluminium foil (grey disc on the right side) and immersed in acetic anhydride and pyridine (4: 3.5 volume ratio) for 1 min followed by heating at 120 $^{\circ}$C for 1 h.
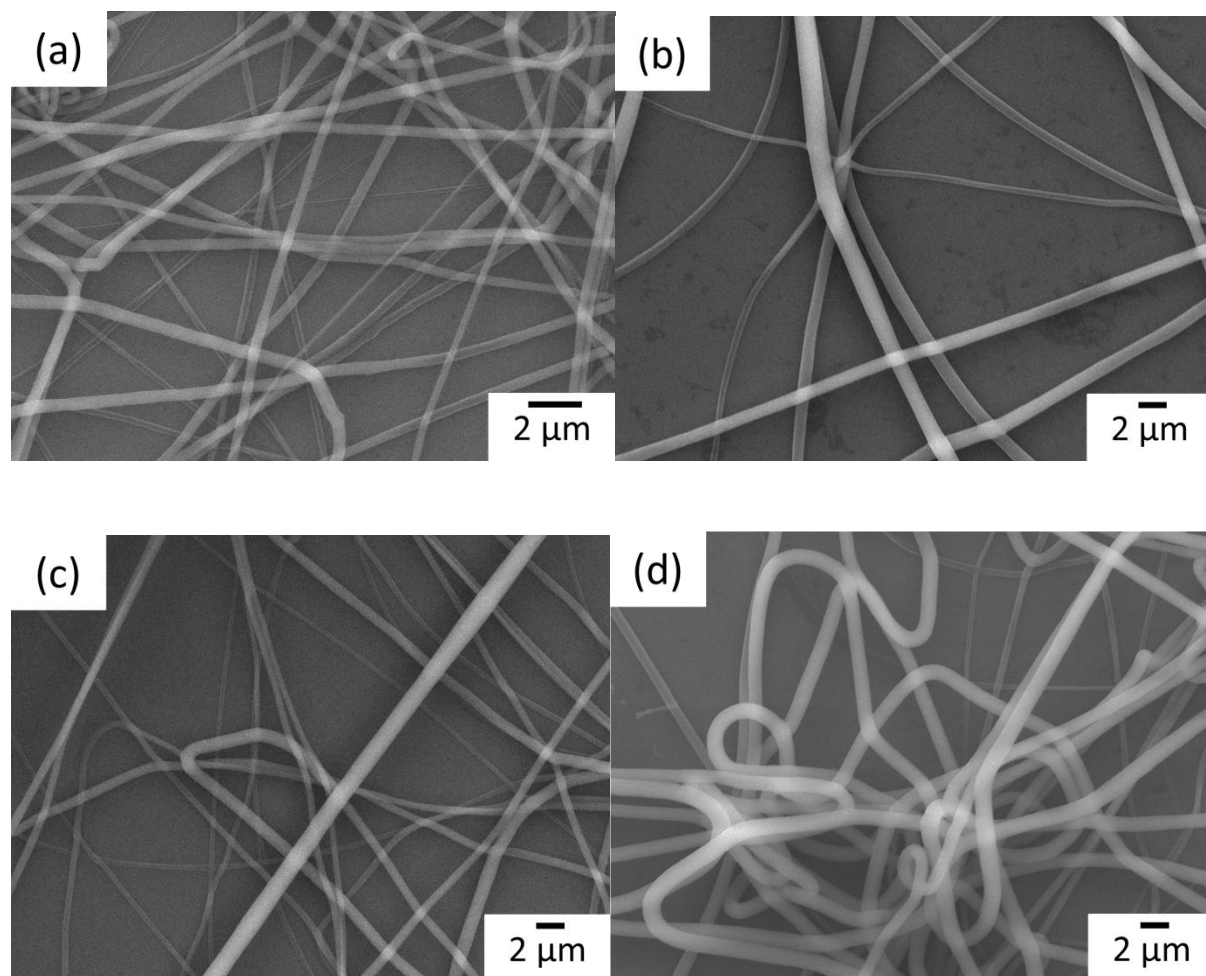
Figure 2. SEM images of pure polyimide fibres electrospun with varied working distance between feeding needle and the collector, (a) 20 cm; (b) 25 cm; (c) 30 cm; (d) 35 cm. Applied voltage of 20 kV, with a feed rate is 0.1 cm^3 h^{-1}; 20 wt% concentration of PI in DMF is 20 wt%. The relative humidity in the electrospinning chamber was 40±5%.
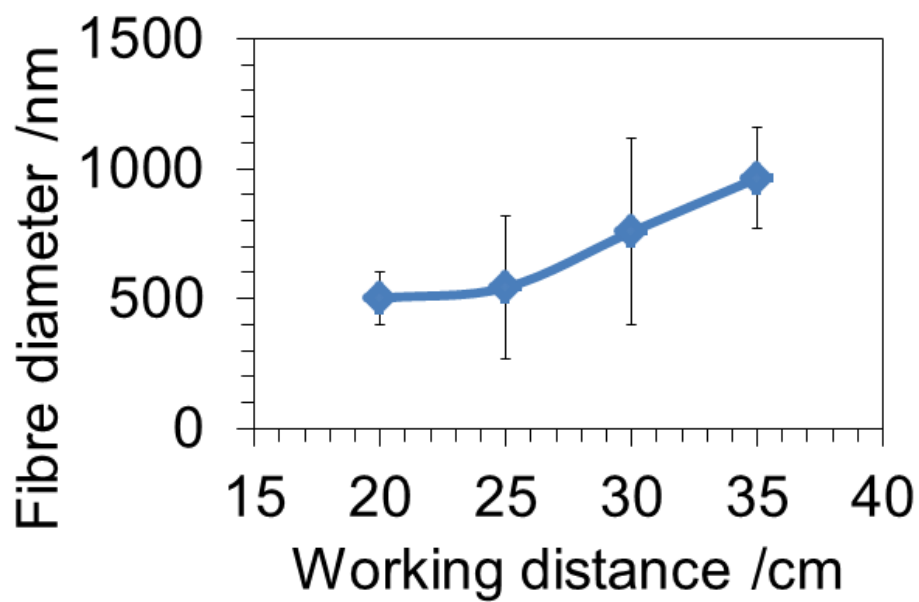
Figure 3. The average diameter of the PI fibres determined from SEM imaging as a function of the working distance between the feeding needle and the collector. Applied voltage of 20 kV, with a feed rate of 0.1 cm^3 h^{-1}; 20 wt% concentration of PI in DMF is 20 wt%. The relative humidity in the electrospinning chamber was 40±5%.
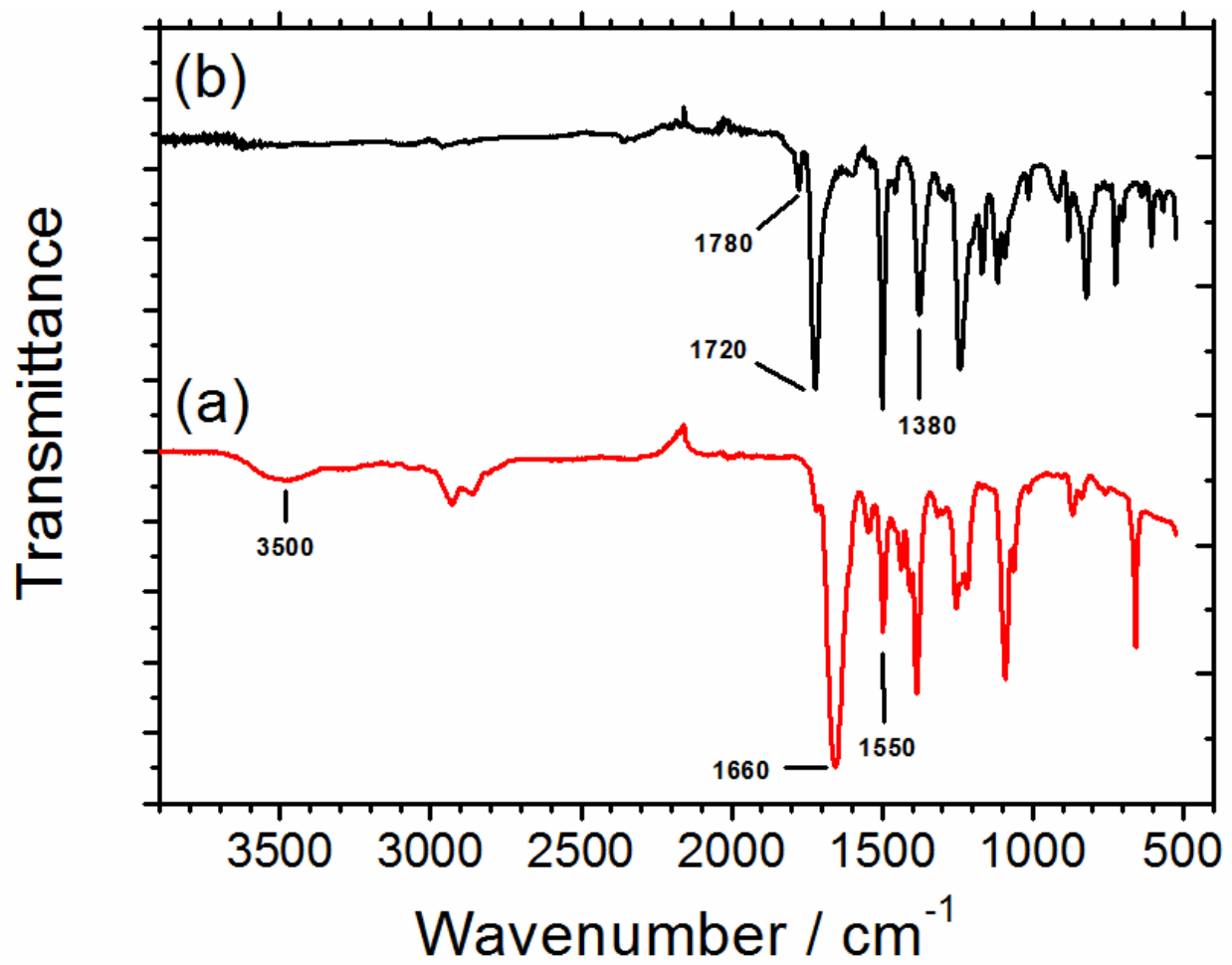
Figure 4. FTIR spectra of neat polymer fibres before and after chemical imidization, (a) polyamic acid; (b) polyimide.
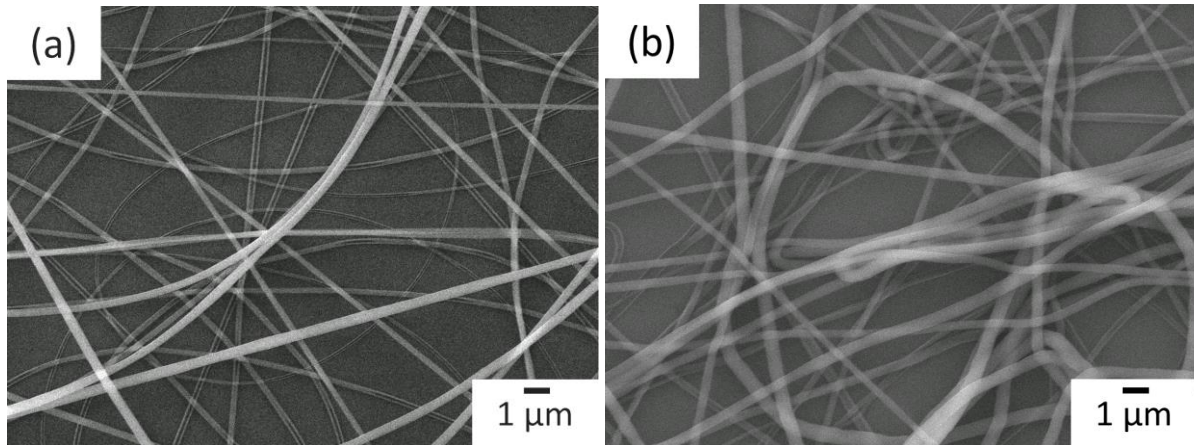
Figure 5. SEM images of electrospun neat polymer fibres before and after chemical imidization (a) polyamic acid fibre and (b) polyimide fibre.
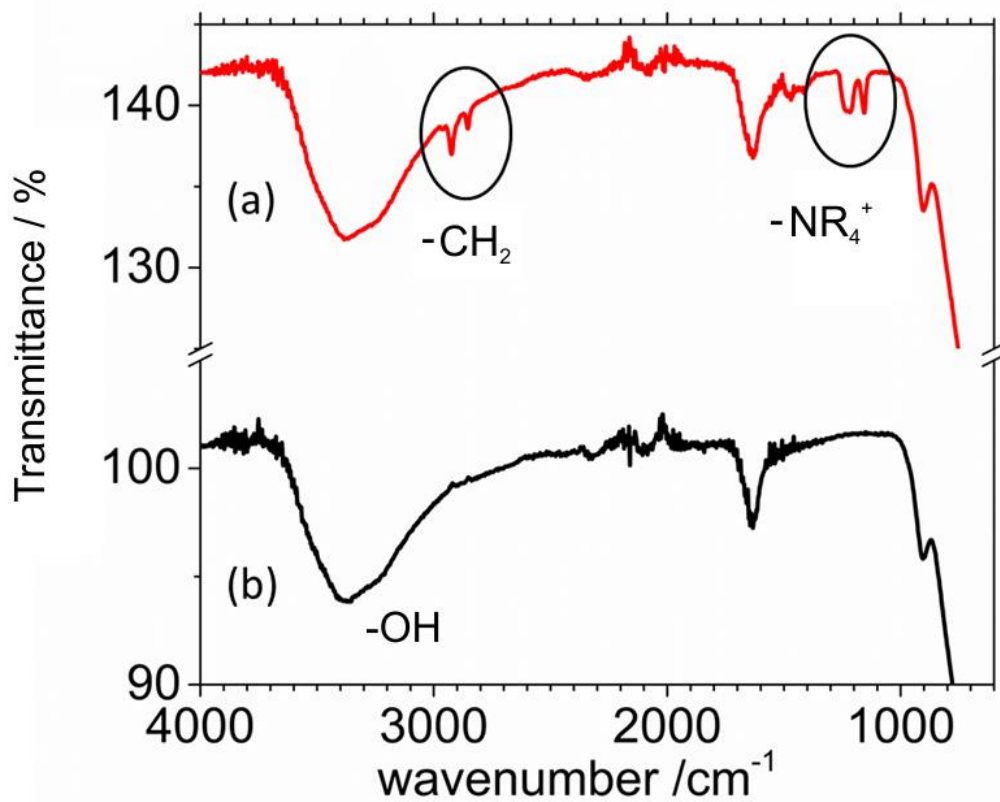
Figure 6. FTIR spectra of (a) CTAB-coated titanate nanotubes and (b) neat titanate nanotubes.
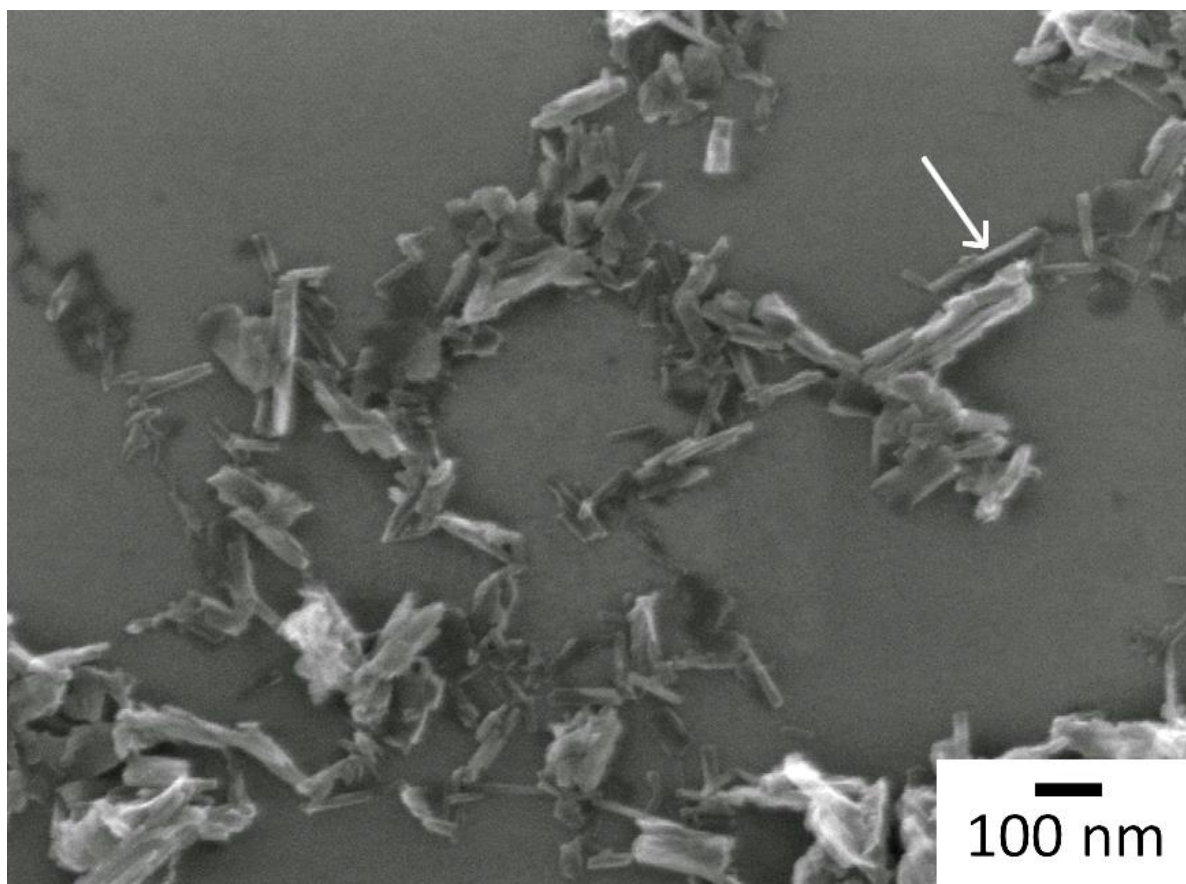
Figure 7. SEM image of CTAB-coated titanate nanotube on the top of silicon wafer after 2 weeks stirring in DMF. The sample was taken from the supernatant from a stable colloidal suspension (240 mg l^{-1}). The arrow indicates an isolated nanotube.
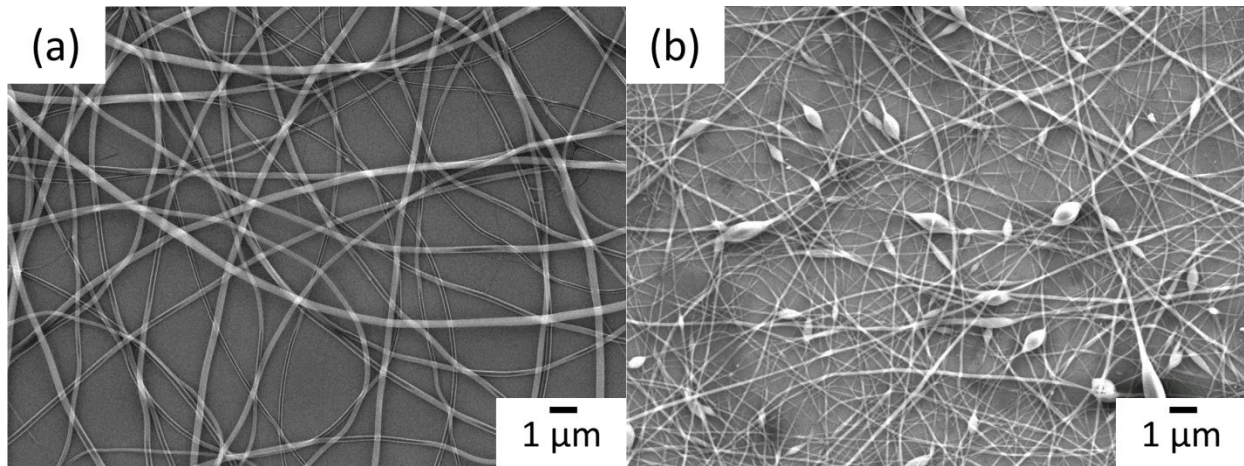
Figure 8. SEM images of polyamic acid-titanate nanotube composite fibre. (a) *ex-situ*

synthesised sample (thick fibre without bead); (b) *in-situ* synthesised sample (thin fibre with

beads).
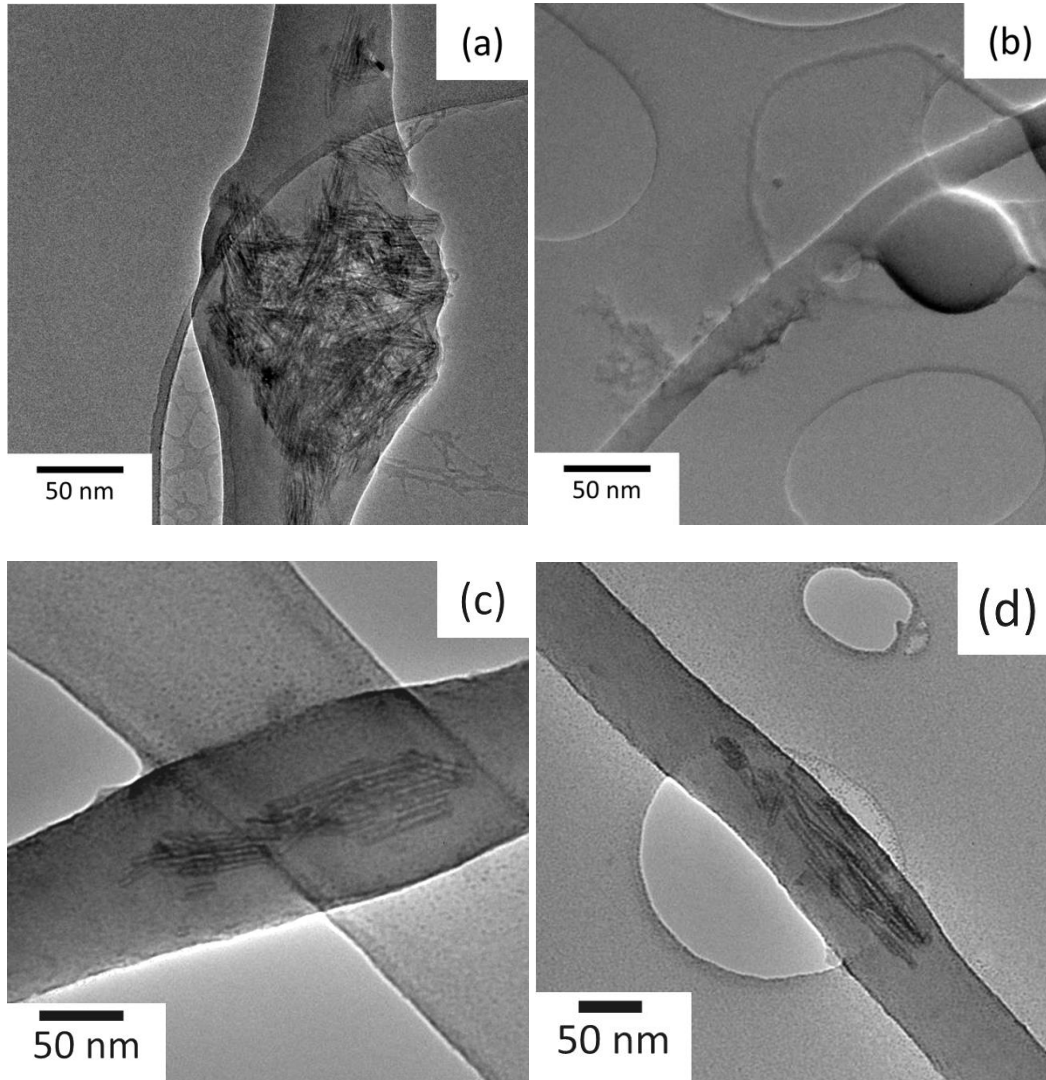
Figure 9. TEM images of electrospun Pi/TiNT composite nanofibres (a) agglomerate of nanotubes within polyimide fibre (after 1 day mechanically stirred sample); (b) empty bead of polyimide (from 2 weeks mechanically stirred sample); (c) aligned nanotubes within polyimide fibre (from *ex-situ* PAA-TINT stable colloidal suspension); (d) aligned nanotubes within polyimide fibre (from *in-situ* PAA-TiNT stable colloidal suspension).
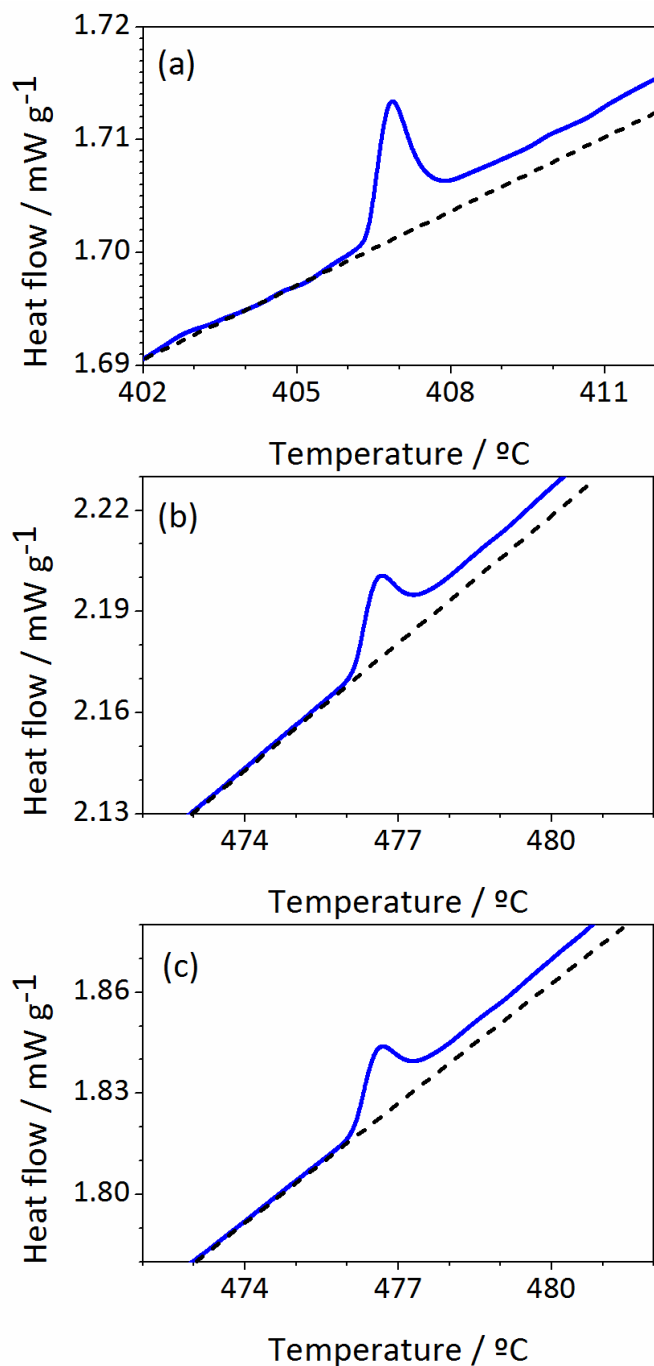
Figure 10. Differential scanning calorimetry (DSC) curves of (a) pure polyimide; (b) *in-situ* synthesized PI/TiNT nanotube composite fibres; (c) *ex-situ* synthesized PI/TiNT nanotube composite fibres. The linear heating rate was 10 ^{o}C min^{-1}.